Extracting coherent coda arrivals from cross-correlations of long period seismic waves during the Mount St. Helens 2004 eruption

Karim G. Sabra,[1] Philippe Roux,[1] Peter Gerstoft,[1] W. A. Kuperman,[1] and Michael C. Fehler[2]

Received 20 December 2005; revised 26 January 2006; accepted 31 January 2006; published 28 March 2006.

[1] We computed cross-correlations of seismic waves generated by Long-Period (LP) events in the frequency band [0.8–2.2 Hz]. The data were recorded in the vicinity of Mount St Helens (MSH) during an eruptive period from September to December 2004. The time symmetric coherent coda arrivals of the time-derivative of the cross-correlation function (DCF), resulting from scattering and topographic effects in MSH area, correspond to arrivals of the Green's function (GF) between the two stations. The DCF waveforms computed on an hourly basis show a remarkable consistency over time periods of several hours but show temporal variations on longer time-scales. We investigated the emergence rate of the symmetric arrivals of the DCF and discussed their potential applications for volcano monitoring. **Citation:** Sabra, K. G., P. Roux, P. Gerstoft, W. A. Kuperman, and M. C. Fehler (2006), Extracting coherent coda arrivals from cross-correlations of long period seismic waves during the Mount St. Helens 2004 eruption, *Geophys. Res. Lett.*, *33*, L06313, doi:10.1029/2005GL025563.

1. Introduction

[2] It has been shown theoretically and experimentally that the time-derivative of the cross-correlation function (DCF) of diffuse wavefields (e.g., ambient noise, scattered waves) recordings on two seismic stations can provide an estimate of a band-limited Green's function (GF) between the stations [*Weaver and Lobkis*, 2001; *Campillo and Paul*, 2003; *Derode et al.*, 2003; *Shapiro et al.*, 2005; *Sabra et al.*, 2005a]. Theory predicts that the resulting DCF should be symmetric in time with positive and negative time components representing propagation paths in opposite directions between the stations [*Wapenaar*, 2004; *Weaver and Lobkis*, 2004]. To date, only body and surface waves components of the GF have been obtained from non-symmetric DCF computed in the ocean microseisms frequency band [*Shapiro et al.*, 2005; *Sabra et al.*, 2005a; *Roux et al.*, 2005]. The lack of time-symmetry was attributed to the directivity of ocean microseisms and relatively weak scattering in the region of observation. In this paper we computed DCF from Long-Period (LP) seismic activity ([0.8–2.2 Hz]) generated by Mount St. Helens (MSH) volcano. As we will discuss below, volcanoes are regions of strong scattering, which make the local LP scattered wavefield more isotropic. Hence we observed: 1) the time-symmetry of coda arrivals of the DCF and 2) long-time scales variations over several days in these symmetric arrivals which may be used as an element of a volcano structural monitoring system independently of the changes in source locations.

[3] Seismic activity sharply increased at MSH during September 2004 after eighteen years of relative quiescence. Five phreatic eruptions occurred from October 1st–5th. Then the seismic activity decreased and transitioned smoothly from high frequency volcano-tectonic events to mostly LP events. A new lava dome grew rapidly in the crater after October 11 and subsequently the LP events became similar and repeatable over several days (Nov. 1–12). The LP sources were located at shallow depth (less than 3km) below the MSH crater [*Dzurisin et al.*, 2005]. The LP seismicity seems connected to the physical changes in the new lava dome [*Moran et al.*, 2005] and thus could be used to characterize MSH structural changes.

[4] Coda arrivals of the LP events likely result from multiple scattering caused by small-scale inhomogeneities in the shallow structure of MSH. Diffusion models applied to earthquake envelopes at Mount Vesuvius predict transport mean free paths l_{tr} as short as 200 m for S-waves in the frequency range 2–20 Hz [*Wegler*, 2003]. In the Earth's crust, over the same frequency range, l_{tr} is 3 orders of magnitude larger: $l_{tr} \sim$100 km [*Margerin et al.*, 1999; *Sato and Fehler*, 1998]. The usefulness of coda waves for studying volcanic systems has been recognized at MSH [*Fehler et al.*, 1988] and for several other volcanoes [*Ratdomopurbo and Poupinet*, 1995; *Aki and Ferrzani*, 2000; *Wegler*, 2003; *Grêt et al.*, 2005]. Over the studied eruptive period September to December 2004 at MSH, more than 500,000 earthquakes up to magnitude 35 have been reported [*Moran et al.*, 2005]. Hence analyzing each LP seismic event separately to study MSH geologic structure is difficult.

[5] Previous volcano monitoring methods included a manual identification of reproducible seismic events recorded at *different* times on a *single* seismic station. Temporal changes in the coda of these events were inferred from waveform cross-correlations [*Ratdomopurbo and Poupinet*, 1995; *Grêt et al.*, 2005]. Here, we process continuous records of all LP events originating from MSH in a given time period which act as multiple random sources of scattered waves. The LP seismicity refers to the whole seismic signals recorded by the stations in the frequency band [0.8–2.2 Hz]. We compute the DCF from LP seismicity recorded at the *same* time on *two* seismic stations to obtain an estimate of the GF. Coherent arrivals emerge from a correlation process that accumulates contributions over time from LP sources whose propagation path pass through both receivers. Hence cross-correlations of LP recordings can be used to infer a band-limited estimate of the GF between station

[1]Marine Physical Laboratory of the Scripps Institution of Oceanography, University of California, San Diego, La Jolla, California, USA.
[2]Los Alamos National Laboratory, Los Alamos, New Mexico, USA.

0094-8276/06/2005GL025563$05.00

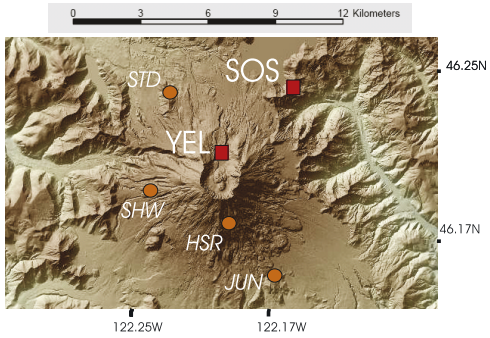

Figure 1. Map view of Mount St Helens Area (source: U.S. Geological Survey). The six closest stations to MSH of the PNSN network are shown.

pairs at MSH without the need for active sources or for processing each LP event individually.

2. Data Processing and Experimental Results

[6] We processed vertical-component data recorded between September 2004 and December 2004 by the six Pacific Northwest Seismic Network (PNSN) stations that are closest to MSH (Figure 1). This network has been extensively used to monitor and image MSH [e.g., *Musumeci et al.*, 2002]. The continuous seismic recordings were first filtered into the dominant frequency band of LP events, 0.8–2.2 Hz, and further homogenized by: 1) keeping only the sign of the resulting time-series (one-bit truncation) to truncate high-amplitude events. This emphasizes wide-angle multiple scattering effects present in the recordings by giving more importance to longer scattering paths that result in late-arriving energy that is smaller in amplitude than the direct arrivals and also increase the contributions of weaker or distant LP sources [*Larose et al.*, 2004], and 2) whitening the data spectrum to diminish eventual spectral peaks (e.g., due to local site effects).

[7] To illustrate the DCF results, the station SOS (north-east of MSH) and YEL (near MSH crater at Yellow Rock), separated by R = 5.49 km, are used because of the favorable orientation of this station pair relative to the strong LP events that occurred south of station YEL. We obtained the DCF(τ, T_r) by processing two data records of length T_r = 3 days (11/03/04–11/05/04), Figure 2a, or T_r = 1h (11/04/04 from 19.00–20.00 GMT), Figure 2b. The normalized DCF(τ, T_r) is obtained after normalization of the DCF amplitude by the standard deviation (Std) of the DCF for large time-delays (70s < $|\tau|$ < 100s). The amplitude of the normalized DCF increases for longer T_r (see Figures 2a and 2b) as theoretically predicted [*Weaver and Lobkis*, 2005; *Sabra et al.*, 2005b]. The envelopes of the coda of the two DCF waveforms resemble those observed at Vesuvius which were modeled using a diffusion equation [*Wegler*, 2003].

[8] When correlating fully diffuse wavefields, the resulting DCF is theoretically proportional to the sum of the negative GF and the time-reversed GF, and its amplitude is a time-symmetric function [*Weaver and Lobkis*, 2004; *Wapenaar*, 2004]. Thus in practice, the portion of the DCF that are time-symmetric can be taken as an estimate of the GF. At MSH, the LP sources are concentrated below the crater and are far from being homogenously distributed around stations SOS and YEL. But this preferential orientation to the seismic sources does not result in a bias in the overall seismic waves propagation direction: the appearance of significant amplitude at both the positive and negative times indicates that backscattering has occurred, most likely from subsurface heterogeneity and surrounding topography (Figure 1), [*Chouet et al.*, 1997; *Sato and Fehler*, 1998; *Snieder*, 2002]. Hence multiple scattering partially compensates for the lack of spatially distributed LP sources to generate diffuse wavefields [*Larose et al.*, 2005]. DCFs for other station pairs also exhibited symmetric coda arrivals, but are not shown here. A measure of the local time-symmetry of the DCF, can be defined by using the correlation coefficient $R(\tau, T_r)$ of the causal ($t > 0$) and anti-causal ($t < 0$) part of the DCF(τ, T_r) over a sliding window of duration $2/B$, where the inverse of the selected bandwidth B = 2.2–0.8 = 1.4Hz is chosen as the temporal resolution of the DCF:

$$R(\tau, T_r) = \frac{\int_{\tau-1/B}^{\tau+1/B} -DCF(t, T_r) \cdot DCF(-t, T_r) dt}{\sqrt{\int_{\tau-1/B}^{\tau+1/B} DCF(t, T_r)^2 dt \int_{\tau-1/B}^{\tau+1/B} DCF(-t, T_r)^2 dt}}$$

[9] Figure 2c (for T_r = 1h) shows an expanded view of the positive and negative time traces plotted on a positive time axis with the maximum DCF amplitude set to 1. Some symmetric arrivals in the DCF that are likely related to true arrivals of the GF, for instance around $\tau \approx$ 5.4s, 9.2s, 13s correspond to high values of $R(\tau, T_r$ = 1h). Other high amplitude arrivals appear in Figure 2c, but only for positive or negative time-delays (e.g., $\tau \approx -11$s, +16.2s) and thus correspond to low values of $R(\tau, T_r$ = 1h), which may be due to bias from LP source locations or insufficient ran-

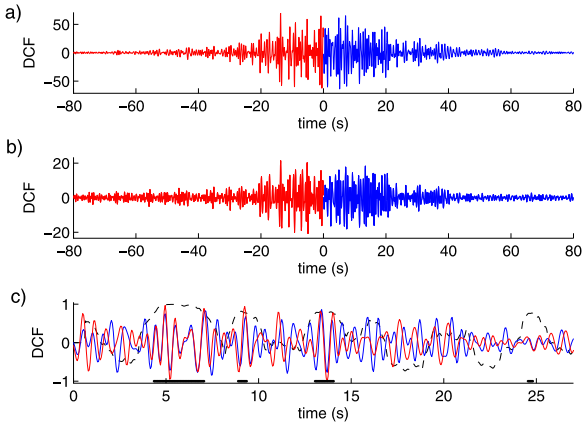

Figure 2. Normalized DCF between stations SOS and YEL obtained by correlations of (a) T_r =3 days of data. (b) Same as Figure 2a but T_r = 1h. (c) Zoom of the superimposed causal (blue line) and time-reversed anti-causal part (red line) of the normalized DCF in Figure 2b. High values (>0.9) of the correlation coefficient $R(\tau, T_r$ = 1h) between the waveforms (black dashed lined) indicate potential GF arrivals-times (thick black lines).

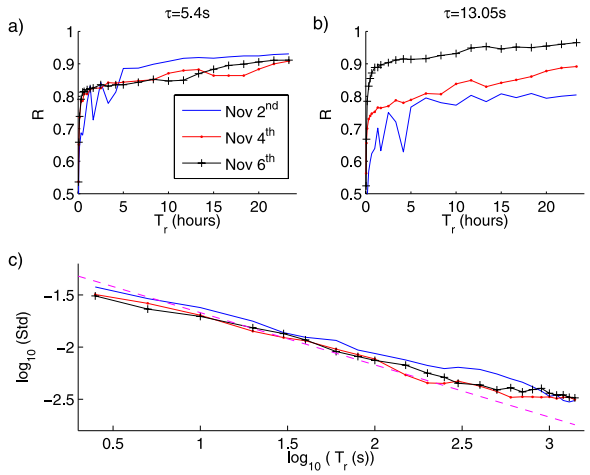

Figure 3. Variations of the average correlation coefficient $R(\tau, T_r)$ (linear scale) vs. the recording duration T_r during 3 different days, for two selected symmetric arrivals (see Figure 2c) centered around (a) $\tau \approx 5.4$s and (b) $\tau \approx 13$s. (c) Standard deviation Std(T_r) value of the DCF in (log scale) and theoretical slope of the Std decay $1/\sqrt{2BT_r}$ (dashed line) for the same days as in Figures 3a and 3b.

domization of the LP events by scattering. Even though these arrivals might be meaningful, the lack of time symmetry of these DCF arrivals prevents a clear identification as a GF arrival.

3. Stability and Emergence Rate of the Symmetric Arrivals of the DCF

[10] The emergence of symmetric arrivals in the DCF depends on the specific spatio-temporal distribution of LP events and scattering at MSH. DCF were computed for increasing duration T_r from 2.5min to 24h. An average DCF(τ, T_r) and correlation coefficient $R(\tau, T_r)$ were computed by averaging results for all distinct time-intervals of duration T_r in a 24h interval. Figure 3 shows R and Std values of the DCF on 3 different days, for two selected symmetric arrivals with similar amplitudes centered around ($\tau \approx \pm 5.4$s and $\tau \approx \pm 13$s), see Figure 2c). The Std of the DCF converges to the actual GF Std, and deviate from it by an amount that decreases like $1/\sqrt{2BT_r}$ as predicted theoretically [*Weaver and Lobkis*, 2005; *Sabra et al.*, 2005b] (see Figures 3c and 3d). On Nov 6th (cross symbols), LP seismicity was steady, hence late arrivals are more symmetric (i.e., higher R) than early arrivals since they likely result from correlation of high order multiply scattered LP events [*Paul et al.*, 2005]. This observation agrees with experimental results showing that multiple scattering and mode conversion helps to attain equipartition in the coda waves [*Campillo and Paul*, 2003; *Larose et al.*, 2005]. However, on Nov 2nd the LP event waveforms varied either due to fluctuations in source processes and locations or GF propagating paths. Consequently, the symmetric coda arrival did not emerge as well in the DCF (plain line) when averaging over longer duration T_r since the multiple scattered effects amplify these fluctuations. Variations on Nov 4th (dotted line) appear as an intermediate case.

[11] Figure 4 displays the envelopes of the energy of the normalized DCF and correlation coefficient R for station-pair SOS-YEL both for T_r = 1h. This duration is small enough to neglect environmental changes in this lapse time but is yet sufficient for the emergence of stable symmetric arrivals in the DCF (see Figures 2c and 3). Important seismic and volcanic events, identified by *Moran et al.* [2005] and *Dzurisin et al.* [2005], are indicated (Events 1–8). Coherent DCF wavefronts start to emerge only after the onset of intense seismic activity on Sept, 23rd (Event 1), at first with low amplitude (below 20dB). The DCF amplitude increases after the extrusion of the new lava dome on Oct, 11th (Event 3). Stability of the LP seismicity (between Event 4 and 5) provides the highest amplitudes over a four week long observation period. A disruption in the coherent arrivals, a lower SNR overall and weak fast arrivals ($\tau < 5$s) occur prior to large swarm of seismic activity (Events 5–7). By inspection of recorded time-series, intense seismic activity (after Event 2,6,7,8) seems to distort the physical response of station YEL located close to MSH crater, thus also lowering the DCF amplitude.

[12] Small medium and source changes are amplified by multiple scattering effects and are easily observed in the coda waveforms [*Sato and Fehler*, 1998; *Grêt et al.*, 2005]. In a scattering environment, symmetric coda arrivals of the DCF correspond to GF arrivals and are independent of the exact locations of LP sources. As long as the time- symmetry persists, as indicated by the correlation coefficient in Figure 4b, a symmetric time-shift of those coda arrivals reflect structural changes of the GF between SOS-YEL and not changes in the LP source locations or processes [*Larose et al.*, 2004]. For instance a symmetric arrival shifted from $|\tau_i| = 9.23$s on Nov 5th to $|\tau_f| = 8.86$s on Nov 11th for both causal and anti-causal parts of the DCF (see white stars on Figures 4a and 4b). This corresponds to an fractional velocity change $\Delta c/c = -(\tau_f - \tau_i)/(\tau_i) = +4\%$ where c is the average velocity along the considered ray path.

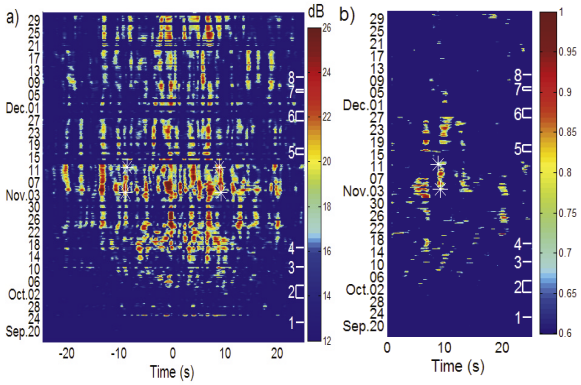

Figure 4. Time-series of (a) energy of the normalized DCF(τ, T_r = 1h) (in dB) and (b) the corresponding correlation coefficient $R(\tau, T_r = 1\text{h})$, from Sept, 18 to Dec, 31 2004. A chronology of seismic events at MSH is indicated: 1) Onset of intense seismic activity (09/23), 2) Phreatic eruptions (10/01–10/05), 3) Extrusion of a new lava dome (10/11), 4) Small lahar (10/17), 5–7) Large cluster of seismic events beneath MSH, 8) First cracks reported on the new dome (12/11).

A uniform motion of the new dome toward the MSH crater rim was observed at the same time [*Moran et al.*, 2005]. This may have created a compression load resulting in the closure of some cracks and changes in the plumbing system below the MSH crater thus modifying the propagation paths between YEL and SOS. The ensuing cluster of large events (Event 5, Nov 16th–18th) caused by the new dome impinging on the south crater wall is consistent with this interpretation. Hence tracking symmetric arrivals of the DCF provides a simple means for monitoring structural changes in scattering environment and does not require the use of similar LP events. Rapid variations in volcanoes have been previously observed using coda wave correlations methods which however require manual identification of reproducible seismic events [*Ratdomopurbo and Poupinet*, 1995; *Grêt et al.*, 2005].

[13] One-sided arrivals may also be used to monitor change, as is evident from the smooth variations in the long streaks in Figure 4a (e.g., $\tau = -13.5$s), when the LP sources appear stable, e.g., time period between Events (4–5) and (5–6). Attributing the shift of these one-sided arrivals to a structural variation of the GF requires additional information, such as events relocation or array beamforming, to further constrain the LP sources locations and directivity.

4. Conclusions

[14] Variations in the time-symmetric coda arrivals of the DCF, occurring within a few days, appear related to physical changes of the new lava dome at MSH. Analyzing the symmetric waveforms of the DCF and their variations could lead to an automatic monitoring technique for structural changes, independently of the changes in source locations. This may help to gain a better understanding of shallow structural heterogeneity as well as the time-scale of the changes in volcanic activity.

[15] **Acknowledgments.** The facilities of the IRIS Data Management System were used for access to waveform and metadata required in this study. We thank C. Rowe and S. Moran for helpful discussions about MSH seismicity, and UCSD-CARE for funding.

References

Aki, K., and V. Ferrzani (2000), Seismic monitoring and modeling of an active volcano for prediction, *J. Geophys. Res.*, *105*, 16,617–16,640.

Campillo, M., and A. Paul (2003), Long-range correlations in the diffuse seismic coda, *Science*, *299*, 547–549.

Chouet, B., G. Saccorotti, M. Martini, P. Dawson, G. De Luca, G. Milana, and R. Scarpa (1997), Source and path effects in the wave fields of tremor and explosions at Stromboli Volcano, *Italy, J. Geophys. Res.*, *102*(B7), 15,129–15,150.

Derode, A., E. Larose, M. Tanter, J. de Rosny, A. Tourin, M. Campillo, and M. Fink (2003), Recovering the Green's function from field-field correlations in an open scattering medium, *J. Acoust. Soc. Am.*, *113*, 2973–2976.

Dzurisin, D., J. W. Vallance, T. M. Gerlach, S. C. Moran, and S. D. Malone (2005), Mount St. Helens reawakens, *Eos Trans. AGU*, *86*(3), 25–36.

Fehler, M., P. Roberts, and T. Fairbanks (1988), A temporal change in coda wave attenuation observed during an eruption of Mount St. Helens, *J. Geophys. Res.*, *93*, 4367–4373.

Grêt, A., R. Snieder, R. C. Aster, and P. R. Kyle (2005), Monitoring rapid temporal changes in a volcano with coda wave interferometry, *Geophys. Res. Lett.*, *32*, L06304, doi:10.1029/2004GL021143.

Larose, E., A. Derode, M. Campillo, and M. Fink (2004), Imaging from one-bit correlations of wideband diffuse wavefields, *J. Appl. Phys.*, *95*, 8393–8399.

Larose, E., A. Derode, D. Clorennec, L. Margerin, and M. Campillo (2005), Passive retrieval of Rayleigh waves in disordered elastic media, *Phys. Rev. E*, *72*, 046607, doi:10.1103/PhysRevE.72.046607.

Margerin, L., M. Campillo, N. M. Shapiro, and B. van Tiggelen (1999), Residence Time of diffuse waves in the crust as a physical interpretation of coda Q: Application to seismograms recorded in Mexico, *Geophys. J. Int.*, *138*, 343–352.

Moran, S., J. W. Vallance, A. I. Quamar, and S. D. Malone (2005), The 2004–2005 eruption of Mount St. Helens: Possible links between seismicity and physical changes in the new lava dome, paper presented at Annual Meeting, Seismol. Soc. of Am., Incline Village, Nev.

Musumeci, C., S. Gresta, and S. D. Malone (2002), Magma system recharge of Mount St. Helens from precise relative hypocenter location of microearthquakes, *J. Geophys. Res.*, *107*(B10), 2264, doi:10.1029/2001JB000629.

Paul, A., M. Campillo, L. Margerin, E. Larose, and A. Derode (2005), Empirical synthesis of time-asymmetrical Green functions from the correlation of coda waves, *J. Geophys. Res.*, *110*, B08302, doi:10.1029/2004JB003521.

Ratdomopurbo, A., and G. Poupinet (1995), Monitoring a temporal change of seismic velocity in a volcano: Application to the 1992 eruption of Mt. Merapi (Indonesia), *Geophys. Res. Lett.*, *22*(7), 775–778.

Roux, P., K. G. Sabra, P. Gerstoft, P. Roux, W. A. Kuperman, and M. C. Fehler (2005), P-waves from cross-correlation of seismic noise, *Geophys. Res. Lett.*, *32*, L19303, doi:10.1029/2005GL023803.

Sabra, K. G., P. Gerstoft, P. Roux, W. A. Kuperman, and M. C. Fehler (2005a), Surface wave tomography from microseism in southern California, *Geophys. Res. Lett.*, *32*, L14311, doi:10.1029/2005GL023155.

Sabra, K. G., P. Roux, and W. A. Kuperman (2005b), Emergence rate of the time-domain Green's function from the ambient noise cross-correlation function, *J. Acoust. Soc. Am.*, *118*(6), 3524–3531.

Sato, H., and M. C. Fehler (1998), *Seismic Wave Propagation and Scattering in the Heterogenous Earth*, Springer, New York.

Shapiro, N. M., M. Campillo, L. Stehly, and M. H. Ritzwoller (2005), High-resolution surface-wave tomography from ambient seismic noise, *Science*, *29*, 1615–1617.

Snieder, R. (2002), Scattering of surface waves, in *Scattering and Inverse Scattering in Pure and Applied Science*, edited by R. Pike and P. Sabatier, pp. 562–577, Elsevier, New York.

Wapenaar, K. (2004), Retrieving the elastodynamic Green's function of an arbitrary inhomogeneous medium by cross correlation, *Phys. Rev. Lett*, *93*, 254301, doi:10.1103/PhysRevLett.93.254301.

Weaver, R. L., and O. I. Lobkis (2001), Ultrasonics without a source: Thermal fluctuation correlations at MHz frequencies, *Phys. Rev. Lett.*, *87*, 134301, doi:10.1103/PhysRevLett.87.134301.

Weaver, R. L., and O. I. Lobkis (2004), Diffuse fields in open systems and the emergence of the Green's function, *J. Acoust. Soc. Am.*, *116*, 2731–2734.

Weaver, R. L., and O. I. Lobkis (2005), Fluctuations in diffuse field-field correlations and the emergence of the Green's function in open systems, *J. Acoust. Soc. Am.*, *117*, 3432–3439.

Wegler, U. (2003), Analysis of multiple scattering at Vesuvius volcano, Italy, using data of the TomoVes active seismic experiment, *J. Volcanol. Geotherm. Res.*, *128*, 45–63.

M. C. Fehler, Los Alamos National Laboratory, Los Alamos, NM 87545, USA.

P. Gerstoft, W. A. Kuperman, P. Roux, and K. G. Sabra, Marine Physical Laboratory of the Scripps Institution of Oceanography, University of California, San Diego, La Jolla, CA 92093-0238, USA. (ksabra@ucsd.edu)